Astronomy & Astrophysics manuscript no. paperII
February 1, 2008

On a multi-resonant origin of high frequency quasiperiodic oscillations in the neutron-star X-ray binary 4U 1636-53

Zdeněk Stuchlík, Gabriel Török, and Pavel Bakala

Institute of Physics, Faculty of Philosophy and Science, Silesian University in Opava,
Bezručovo nám. 13,CZ-74601 Opava, Czech Republic

Received / Accepted

ABSTRACT

Context. The kHz quasiperiodic oscillations (QPOs) observed in low-mass X-ray neutron star binaries are most likely connected to the orbital motion in the accretion disc. The ratio between frequencies of the upper and lower observed QPOs mode cluster close to ratios of small natural numbers, most often close to the 3/2 value, but the other rational ratios occur in some sources as well. The class of QPOs models considers a resonance between Keplerian and epicyclic frequencies of the geodesic motion. It was suggested that a multipeaked ratio distribution may follow from different resonances. The atoll source 4U 1636-53 shows datapoints clustering around two distinct values (3/2 and 5/4) of the frequency ratio. The same frequency ratios correspond to the change in the sign of the twin peak QPOs amplitude difference, suggesting existence of a resonant energy overflow.
Aims. We explore the idea that the two clusters of datapoints in 4U 1636-53 result from two different instances of the same orbital resonance corresponding to the two resonant points.
Methods. Assuming the neutron star external spacetime to be described by the Hartle-Thorne metric, we search for a frequency relation, matching the two observed datapoints clusters, which may correspond to a resonance. We consider orbital and associated epicyclic frequencies with accuracy up to the second order terms in the neutron star angular momentum j and first order terms in its quadrupole moment q.
Results. We have identified a suitable class of frequency relations well fitting the observed data. These models imply for central compact object in 4U 1636-53 the mass $M = 1.6-2.5M_{\odot}$, dimensionless angular momentum $j = 0-0.4$, and quadrupole momentum $q = 0-0.25$, with most preferred values $M \doteq 1.77M_{\odot}$, $j \doteq 0.05$, and $q \doteq 0.003$.
Conclusions. The relationship implied for a particular case of so called total precession resonance between the Keplerian and the total precession frequency introduced in this paper resembles the twin peak QPOs observed in 4U 1636-53 with a $\chi^2 \sim 3\,d.o.f.$ which is about one order lower than χ^2 reached by other theoretical relationships which we examine. Moreover, the position of 3/2 and 5/4 resonant points implied by the total precession relationship well coincides with frequencies given by the change of the rms-amplitude difference sign. Notice that if a resonance (in our opinion most likely present) is not considered, the total precession relation has a similar kinematic meaning as the periastron precession relation involved in the model of Stella and Vietri, but gives substantially better fit and lower neutron star mass.

Key words. X-ray variability – observations – theory – 4U 1636-53

1. Introduction

Rossi X-ray Timing Explorer (RXTE, Bradt et al., 1993) provides observations of the high frequency kilohertz QPOs in the X-ray fluxes from neutron-star binary systems (see, van der Klis, 2006, for a review).

Several models have been outlined to explain the kHz QPO frequencies, and it is mostly preferred that their origin is related to the orbital motion near the inner edge of an accretion disc. In particular, two ideas based on the strong gravity properties have been proposed. While Stella & Vietri (1998, 1999) introduced the "Relativistic Precession Model" in which the kHz QPOs represent direct manifestation of the modes of a relativistic epicyclic motion of blobs in the inner parts of the accretion disc, Kluźniak & Abramowicz (2001) proposed models based on resonant interaction between orbital and/or epicyclic modes related to nonlinear oscillations of the accretion disc.

Abramowicz et al. (2003) noticed that ratio between the frequencies ν_L and ν_U of the lower and upper observed kHz QPO mode cluster in neutron-star sources usually close to ratios of small natural numbers, most often close to the value $\nu_U/\nu_L = 3/2$.[1] The ratio clustering was later confirmed by Belloni et al. (2005). The question whether such a clustering represents clear argument supporting a resonance hypothesis remains to be subject of discussions. Nevertheless it was also suggested that, due to multipeaked distribution in the frequency ratio, more than one resonance could be at work if a resonant mechanism is involved in generating the neutron-star (Belloni et al., 2005; Török et al., 2007) and black-hole (Stuchlík & Török , 2005) kHz QPOs.

Török & Barret (2007) realized an interesting root-mean-squared-amplitude (rms amplitude) evolution in group of six neutron star atoll sources (namely 4U 1636-53, 4U 1608-52, 4U 1820-30, 4U 1735-44, 4U 1728-34 and 4U 0614+09) - the upper and lower QPO amplitudes equal each other when the source passes through a rational frequency ratio. Such a behaviour highly suggests the existence of an energy overflow be-

Send offprint requests to: G. Török, terek@volny.cz

[1] The same 3/2 ratio of QPO frequencies was first noticed in the GRO J1655-40 data by Abramowicz & Kluźniak (2001) and later found in all other microquasars in which the twin QPOs have been detected (see, McClintock & Remillard, 2004).

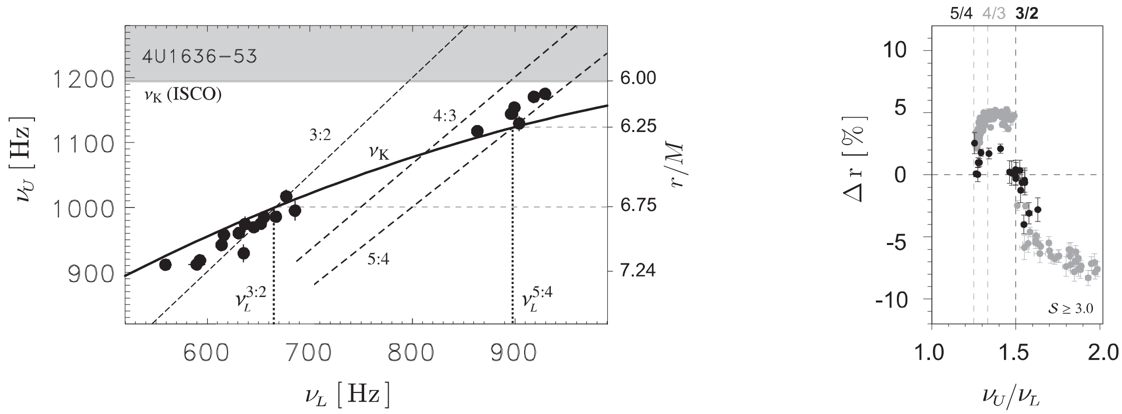

Fig. 1. Left (from Török et al., 2007): The frequency correlation in the atoll source 4U 1636-53. Curve ν_K determines the upper QPOs frequency following from the relativistic precession model (Stella & Vietri, 1999) under the consideration of the gravitational field described by the Schwarzschild metric with the central mass $M = 1.84M_{\odot}$. The secondary vertical axes indicates the appropriate dimensionless radius. One should note that the assumed 5:4 resonance occurs very close ($0.25M$) to the *innermost stable circular geodesic orbit*, i.e., near the expected inner edge of the accretion disc. Right (from Török & Barret, 2007): The rms amplitude difference as a function of the frequency ratio in 4U 1636-53 (black points). Gray points correspond to the single detections of the lower (upper) QPOs and the absolute value of their rms amplitude.

tween the upper and lower frequency mode typical for non-linear resonances. The effect seems to be related to the results of the frequency ratio distribution studies because the change of the rms amplitude difference sign occurs close to the same frequency ratio as those corresponding to the datapoints clustering.

The results of studies mentioned above indicate that for a given source the upper and lower QPO frequency can be traced through the whole observed range of frequencies but the probability to detect both QPOs simultaneously increases when the frequency ratio is close to the ratio of small natural numbers (namely 3/2, 4/3 and 5/4 in the case of six atoll sources, Török & Barret, 2007).

Figure 1 illustrates the frequency correlation for the atoll source 4U 1636-53 together with its rms amplitude difference evolution.[2] For the 3/2 and 5/4 frequency ratio the two distinct clusters of datapoints are easy to recognize on the figure as well as the corresponding change of the rms amplitude difference sign.

In this paper we focus on 4U 1636-53 and explore the idea (Török et al., 2007) that the two clusters of datapoints mentioned above result from two different instances of the same orbital resonance varying in resonant coefficients.

2. Orbital frequencies of geodesic motion close to rotating neutron stars

In Newtonian physics, a test particle orbits the central mass M with the Keplerian angular velocity $\Omega^* = (GM/r^3)^{1/2}$ and its, in general eliptic, trajectory is closed, i.e., related *azimuthal (or Keplerian)* ν_K^*, *radial* ν_r^*, and *vertical* ν_θ^* orbital frequencies equal each other.

In the general relativistic description, necessary in the case of compact objects inluding neutron stars (Misner et al., 1973; Shapiro & Teukolsky, 1986; Glendenning, 1997), the trajectory of a test particle is not closed and the frequencies of the azimuthal, radial and vertical "quasielliptic" orbital motion differ. For a given axially symetric spacetime with the line element

$$\mathrm{d}s^2 = g_{tt}\,\mathrm{d}t^2 + g_{rr}\,\mathrm{d}r^2 + g_{\theta\theta}\,\mathrm{d}\theta^2 + g_{\phi\phi}\,\mathrm{d}\phi^2 + g_{\phi t}\,\mathrm{d}\phi\,\mathrm{d}t + \\ + g_{t\phi}\,\mathrm{d}t\,\mathrm{d}\phi\,, \tag{1}$$

the relevant angular velocities read (e.g., Aliev & Galtsov, 1981; Okazaki et al., 1987; Stella & Vietri, 1998; Abramowicz et al., 2003a)[3]

$$\Omega_{\mathrm{K}} = u^{\phi}/u^{t}, \tag{2}$$

$$\omega_{\mathrm{i}}^2 = \frac{(g_{tt} + \Omega_{\pm}\, g_{t\phi})^2}{2g_{\mathrm{ii}}} \left(\frac{\partial^2 U}{\partial \mathrm{i}^2}\right)_{\ell}, \tag{3}$$

where $\mathrm{i} \in (r, \theta)$ and U is an *efffective potential*

$$U(r, \theta, \ell) := g^{tt} - 2\ell\, g^{t\phi} + \ell^2\, g^{\phi\phi}, \tag{4}$$

with ℓ denoting the specific angular momentum of the orbiting test particle

$$\ell = -u_{\phi}/u_{t}\,. \tag{5}$$

In the following we consider Keplerian motion and $l = l_K(r, \theta)$. The motion is then described by the Keplerian frequency ν_K and radial and vertical epicyclic frequencies $\nu_{\mathrm{r}},\ \nu_{\theta}$.

Due to the inequality between the azimuthal and radial frequency, the eccentric orbits waltz at the *periastron precession frequency* (e.g., Misner et al., 1973)

$$\nu_{P} = \nu_{K} - \nu_{\mathrm{r}}, \tag{6}$$

and in addition the orbits tilted relative to the equatorial plane of the spinning central mass wobble at the *nodal (often called Lense–Thirring) precession frequency* (e.g., Misner et al., 1973)

$$\nu_{LT} = \nu_{K} - \nu_{\theta}. \tag{7}$$

The periastron precession frequency (6) corresponds to the period in which the test particle "quasielliptic" trajectory periastron oscillates and the nodal (Lense-Thirring) precession frequency (7) corresponds to the period in which the declination

[2] The data (Barret et al., 2005; Abramowicz et al., 2005) correspond to individual continuous segments of observation processed by standard shift–add technique (see, Méndez et al., 1998). Notice that some other methods, namely shift-add through all segments of data (see, Barret et al., 2005), provide more efficient analysis of the frequency correlation but do not keep the information about the probability of the detection (i.e., the frequency distribution).

[3] In the text above we mark the frequencies expressed in standard (SI) physical units by asterisk. Hencefort we already use the geometrical units ($c = 1 = G$; $M = GM^*/c^2$, $r = r^*$, $t = ct^*$).

of the quasiellipse plane oscillates. Both the declination of the quasiellipse plane and position of the periastron then reach the initial state simultaneously in the period characterized by the frequency

$$\nu_T = \nu_P - \nu_{LT} = \nu_\theta - \nu_{\mathrm{r}}. \tag{8}$$

Therefore, for the purposes of our paper, we call this frequency *total precession frequency*. [4]

2.1. The Hartle-Thorne metric

In this paper we describe the external neutron star spacetime using the Hartle-Thorne metric (Hartle & Thorne, 1968) which represents the exact solution of vacuum Einstein field equations for the exterior of rigidly and relatively slowly rotating, stationary and axially symmetric body. The metric is given with accuracy up to the second order terms in the body's dimensionless angular momentum $j = J/M^2$, and first order in its dimensionless quadrupole moment $q = -Q/M^3$. The explicit form of formulae (2) and (3) derived by Abramowicz et al. (2003a), which we use in a slightly modified form, is given in Appendix A.

3. Testing the multiresonant hypothesis

3.1. Frequency identification

Usually the $n : m$ orbital resonant models considering a non-linear resonance between Keplerian and/or epicyclic frequencies (see, e.g. Abramowicz et al., 2004) identify the resonant eigenfrequencies $\nu^0_L,\ \nu^0_U$ as

$$\nu^0_L = \nu_{\mathrm{r}}(r_{n:m}),\ \nu^0_U = \nu_{\mathrm{v}}(r_{n:m}),\ \ \nu_{\mathrm{v}} \in [\nu_\theta,\ \nu_K] \tag{9}$$

where n, m are small natural numbers and $r_{n:m}$ is the radius fixed by the condition

$$\frac{\nu_{\mathrm{v}}(r_{n:m})}{\nu_{\mathrm{r}}(r_{n:m})} = \frac{n}{m}. \tag{10}$$

In the case of a considerably weak forced or parametric non-linear resonance (Landau & Lifshitz, 1976), the upper and lower observed QPO frequencies ν_L and ν_U are related to the resonant eigenfrequencies either directly

$$\nu_L \doteq \nu^0_L, \quad \nu_U \doteq \nu^0_U, \tag{11}$$

or as their linear combinations

$$\nu_L \doteq \alpha\nu^0_L, \quad \nu_U \doteq \beta\nu^0_U, \tag{12}$$

where α and β are small integral numbers. This property was utilized to estimate the spin of microquasars displaying constant twin peak QPOs from resonant models (Abramowicz & Kluźniak, 2001; Török et al., 2005).

In general case of a system in a non-linear resonance, the observed frequencies differ from resonance eigenfrequencies by a frequency corrections proportional to the square of small dimensionless amplitudes (Landau & Lifshitz, 1976). It was shown (Abramowicz et al., 2003b; Rebusco, 2004) that a resonance characterized by one pair of eigenfrequencies may reproduce the whole range of frequencies observed in a neutron star source. Later Abramowicz et al. (2005) considered the idea of one eigenfrequency pair (so called resonant point in the frequency-frequency plane) common for a set of neutron star sources. They shown that for weakly coupled non-linear resonance the upper and lower frequency observed in a source should be linearly correlated. They also found that coefficients of linear fits well approximating individual sources are anticorrelated which was in a good accord to the theory they presented and justified the hypothesis of one eigenfrequency-pair. On the other hand this approach, incorporating certain difficulties (e.g., the extremely large extension of the observed frequency range), is not proved yet, and some observational facts like the multipeaked ratio distribution suggest that more then one resonant points may be responsible for the almost linear observed frequency correlation.

In next *we focus on the hypothesis of more resonant points corresponding to different instances of one resonance and suppose that the observed frequencies are close to the resonance eigenfrequencies, i.e. that the observed frequency correlation follows the generic relation between resonant eigenfrequencies*,

$$\nu_L \sim \nu^0_L, \quad \nu_U \sim \nu^0_U. \tag{13}$$

For the whole applicable range of the internal angular momentum j of the Hartle-Thorne spacetimes we checked that the ratio between the Keplerian (or vertical epicyclic) frequency and radial epicyclic frequency monotonically increases with decreasing radius r whereas the Keplerian (vertical epicyclic) frequency increases (see also Török & Stuchlík, 2005).

In other words, *for the models (9) considering resonance between Keplerian (vertical epicyclic) frequency and radial epicyclic frequency satisfying relation (13), the ratio of observed frequencies should increase with increasing QPO frequency, but that is opposite to what is observed*.

However, the relations (10–12) are not the only possible in the framework of resonance models. Bursa (2005) discussed so called vertical precession resonance introduced in order to match the spin estimated from fits of the X-ray spectral continua for the microquasar GRO J1655-40. The resonance should occur between the vertical epicyclic frequency and the periastron precession frequency fulfilling the relation

$$\nu^0_L(r) = \nu_P(r) = \nu_K(r) - \nu_{\mathrm{r}}(r), \quad \nu^0_U(r) = \nu_\theta(r), \tag{14}$$

for a particular choice of the resonant radius r defined by the condition $\nu_{\mathrm{u}} = 3/2\nu_{\mathrm{l}}$.

As noticed in Török et al. (2007), for the Schwarzschild spacetime the relations (14) coincide with those following from the relativistic precession model:

$$\nu^0_L(r) = \nu_P(r) = \nu_K(r) - \nu_{\mathrm{r}}(r), \quad \nu^0_U(r) = \nu_K(r). \tag{15}$$

Opposite to the relations (9) the two relationships (14,15) as well as the other two relationships

$$\nu^0_L(r) = \nu_\theta(r) - \nu_{\mathrm{r}}(r), \qquad \nu^0_U(r) = \nu_\theta(r), \tag{16}$$

$$\nu^0_L(r) = \nu_T(r) = \nu_\theta(r) - \nu_{\mathrm{r}}, \quad \nu^0_U(r) = \nu_K(r) \tag{17}$$

imply the increase of ν^0_U for increasing ν^0_L.

In the following subsection we fit the QPO frequencies observed in 4U 1636-53 by the four different frequency relationship (14–17), testing the hypothesis that an appropriate resonance may be responsible for all the observed datapoints.

3.2. Individual fits

The fits are realized in two steps. In order to obtain a rough scan we calculated frequency relations (14–17) in the Hartle–Thorne metric for the range of the mass $M \in 1$–$3M_\odot$, the internal angular momentum $j \in 0$–0.5 and a physically meaningful

[4] Note that in general the repeating of initial periastron position and orbit declination do not guarantee repeating of the initial test particle position at the same time.

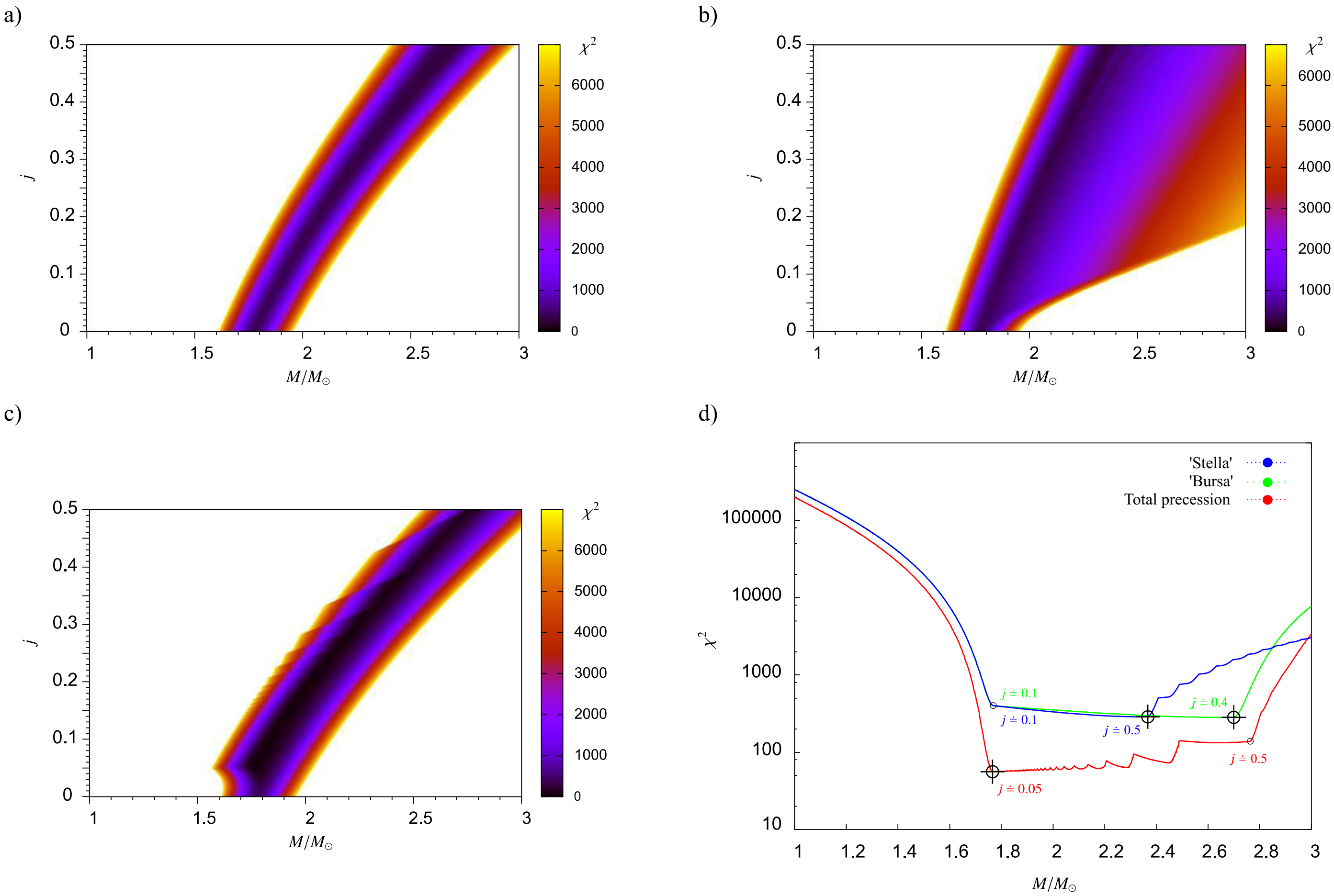

Fig. 2. a) The inverse quality measure χ^2 of the datapoints fits by relation (15) – "Stella" as a function of the neutron star mass M and the angular momentum j. The displayed individual values of χ^2 correspond to the quadrupole momentum q giving the best fit for the fixed pairs $(M,\ j)$. b) The same for the relation (14) – "Bursa". c) The same but for the relation (17) – total precession. For all the three relations, the χ^2 minima form "valleys" with rather sharp roots. d) Profiles of the individual valleys. The cross-hair marks denote the value of the global minima. For relations "Stella" and "Bursa" the value of χ^2 local minimum at the bottom of the valley decreases with the increasing angular momentum j. On the other hand for the total precession relation it increases with the increasing angular momentum j.

quadrupole momentum q with a step equivalent to the thousand points in all three quantities, i.e., four 3-dimensional maps each having 10^9 points. Then, for each pair (M, j), we keep the value of the quadrupole momentum q which gives the lowest χ^2 with respect to the observed datapoints. For the Schwarzschild spacetime ($q = j = 0$), when relations (14–17) merge, the best fit is reached for the mass $M \doteq 1.77 M_{\odot}$, with a $\chi^2 \doteq 400 \sim 20\, d.o.f.$ Because for rotating configurations the relation (16) gives rather less interesting results, we do not consider this relation in the following.

Figures 2 a, b, and c show the lowest χ^2 associated with relations (15) – "Stella", (14) – "Bursa", and (17) – total precession, for each pair (M, j). Having a rough clue given by Figures 2a,b, and c we searched for local χ^2 minima using the Marquardt–Levenberg non-linear least squares method (Marquardt, 1963). Particular minima we have found are denoted in Figure 2d.

The detailed analysis shown that both the relations (14) and (15) match the observational data most likely for relatively high angular momentum close to $j \sim 0.5$ and the central mass $M \sim 2.4$–$2.8 M_{\odot}$ ("Stella"), and $M \sim 2.4 M_{\odot}$ ("Bursa") respectively, reaching the value of $\chi^2 \sim 15\, d.o.f.$, whereas the quadrupole momentum is rather close to the Kerr value $q = a^2 = j^2$ ($q \sim 0.23,\ 0.25$).

Relation (17, total precession) gives the best fit with the remarkable $\chi^2 \sim 3\, d.o.f.$ for angular momentum $j \sim 0.05$ and central $M \sim 1.76\, M_{\odot}$, again with the quadrupole momentum close to the Kerr value ($q \sim 0.029$)[5]. For this relationship the quality of the fit is then very close to $\chi^2 \sim 3\, d.o.f.$ in rather large range of the central mass $M \sim 1.76$–$1.84 M_{\odot}$ and the angular momentum $j \sim 0.05$–0.1.

4. Discussion and conclusions

Figures 3a,b, and c show the best fits reached by relations (14–17). The relevant best fits properties are summarized in the Table 1. Apparently, the identification of the lower kHz QPOs with total precession frequency and the upper kHz QPOs with the Keplerian frequency[6]

$$\nu^0_L(r) = \nu_T(r) = \nu_\theta(r) - \nu_r(r), \qquad \nu^0_U(r) = \nu_K(r)$$

reaches a substantially better quality of the fit ($\chi^2 \doteq 3\, d.o.f.$) then the other three possibilities. The corresponding value of

[5] Our results are thus compatible with expectation that gravitational field of settled down neutron stars can be well described by quasi-Kerr spacetime.

[6] As previously stressed, our paper focuses on the hypothesis of one resonance which occurs at different resonant points. The more general multiresonant idea, including the possibility of several resonances sharing the common radius, relevant for compact objects with special values of the angular momentum, is discussed in Stuchlík et al. (2007).

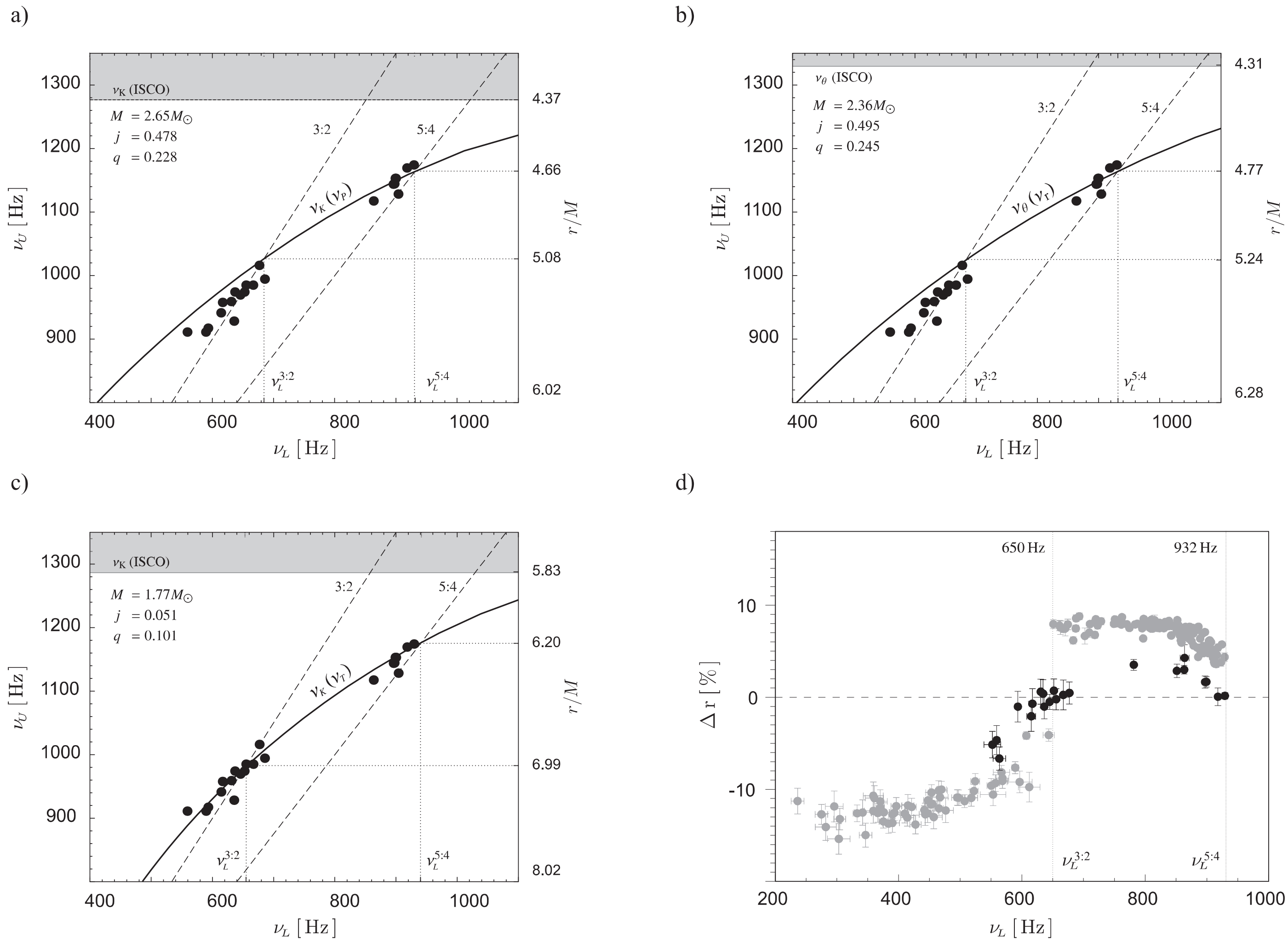

Fig. 3. a) The best fit by relation (15) – "Stella". b) The best fit by relation (14) – "Bursa". c) The best fit by relation (17) – total precession. d) Adopted from Török & Barret (2007). The difference of the lower and upper QPOs rms amplitudes plotted as a function of the lower QPOs frequency (black points). Assuming zero amplitude of the missing QPOs mode, the quantity Δr is for single peaks (grey points) given by an absolute value of their rms amplitude. To plot Δr corresponding to the upper single QPO we used the linear frequency–frequency fit. Dotted vertical lines denote position of the qualitative change in the rms amplitude interrelationship.

the angular momentum $j \sim 0.05$–0.1 and mass $M \sim 1.8$ are not excluded by any study published so far (Strohmayer & Markwardt, 2001; Giles et al., 2002) and this frequency identification appears more likely than the relationship corresponding to the relativistic precession model of Stella & Vietri ($M \sim 2.4$–$2.8M_\odot$, $j \sim 0.4$–0.5).

The total precession frequency ν_T given by (8) corresponds to the period in which the declination of the free test particle quasiellipse plane and the periastron reach simultaneously the initial state. Consideration of a hot spot with characteristic frequencies (17) may represent a kinematic QPOs model very close (but obviously not identical) to those of Stella & Vietri.[7]

However, the observed ratio clustering and rms amplitude difference behaviour suggest the existence of a resonance between the lower and upper QPOs modes. Notice also that the position of the 3/2 and 5/4 resonant points implied by the total precession relationship (i.e., intersections of the best datapoints fit with reference 3/2 and 5/4 lines) well coincide with frequencies given by the change of the rms-amplitude difference sign (see Figure 3 and Table 1). Therefore, our results indicate that the resonance may occur between the Keplerian frequency of the trajectory and the total precession frequency corresponding to the periodicity of the trajectory shape.[8] The concrete physical mechanism of such a resonance remains to be the subject of a future and rather larger research since, beyond the hotspot interpretation, the Keplerian and total precession frequency may also correspond to some disk oscillation modes.

The results we have obtained so far indicate that Keplerian and total precession frequency (17) match the kHz QPOs frequencies very well at least in several atoll sources (Bakala et al., 2007, in preparation).

On the other hand, the applicability of the relation (17) to the Galactic microquasar sources poses an open question because it implies the central black hole spin similar to those of Stella & Vietri ($a \sim 0.3$–0.5), which in the case of microquasar GRS 1915+105 contradicts the recent results of a fitting the spectral continua ($a \sim 0.7$–1, McClintock et al., 2006; Middleton et al., 2006).

[7] One may also argue that if the light curve is somehow simultaneously modulated by the periastron and Lense-Thirring precession, the beat frequency should appear in its power spectra.

[8] For the perfect free particle motion, if the Keplerian and total precession frequency form rational fractions, the trajectory is selfrepeating (i.e., closed).

Table 1. The properties of best fits depicted in Figure 3a,b, and c (in the case of the totall precession we display also properties of the fit for the angular momentum $j \doteq 0.1$). The uncertainities in the fit parameters are the standard $\chi^2 + 1$ errors. Quantity Δq characterizes the deviation of the quadrupole momentum from the value corresponding to the Kerr spacetime. Quantities $\Delta\nu_L$ characterize the deviation of best fit intersections with reference 3/2 and 5/4 lines from the value given by the qualitative change in the rms amplitudes behaviour.

Model		Best fit					Resonant points						
ν_L	ν_U	M	j	q	Δq	$\frac{\chi^2}{d.o.f.}$	$\frac{r_{3:2}}{M}$	$\frac{\nu_L^{3/2}}{\text{Hz}}$	$\frac{r_{5:4}}{M}$	$\frac{\nu_L^{5/4}}{\text{Hz}}$	$\frac{\Delta\nu_L^{3/2}}{\text{Hz}}$	$\frac{\Delta\nu_L^{5/4}}{\text{Hz}}$	$\frac{\overline{\Delta\nu_L}}{\text{Hz}}$
"Stella"													
ν_P	ν_K	2.65±0.20	0.478±0.099	0.228±0.096	0.000	15	5.08	684	4.66	931	34	1	17.5
"Bursa"													
ν_P	ν_θ	2.36±0.01	0.495±0.005	0.245±0.004	0.000	15	5.24	683	4.77	931	33	1	17.0
Total precession													
ν_T	ν_K	1.77±0.07	0.051±0.044	0.003±0.009	0.0003	3	6.99	655	6.20	940	5	8	6.5
Total precession													
ν_T	ν_K	1.84±0.08	0.101±0.044	0.011±0.009	0.0001	3	6.8	653	6.01	941	3	9	6.0

Acknowledgments

The authors have been supported by the Czech grants MSM 4781305903 (ZS and GT) and LC 06014 (PB).

References

Abramowicz, M.A., Kluźniak, W., A&A, v.374, p.L19–L20 (2001)
Abramowicz, M.A., Bulik, T., Bursa, M., Kluźniak, W., 2003, A& A, 404, L21
Abramowicz, M.A., Almergren, G.J.E., Kluźniak, W., Thampan, A.V., astro-ph/0312070
Abramowicz, M. A., Karas, V., Kluzniak, W., Lee W. H., Rebusco, P., 2003, PASJ, Vol.55, No.2, pp. 467–466
Abramowicz, M.A., Kluźniak, W., Stuchlík, Z., Török, G., in Proceedings of RAGtime 5, Opava, 2004, p. 1–24
M. A. Abramowicz, D. Barret, M. Bursa, J. Horák, W. Kluźniak, P. Rebusco, and G. Török, in Proceedings of RAGtime 6/7, Opava, 2005
A. N. Aliev, D. V. Galtsov, GRG, 1981, 13, p. 899
Bakala P., Török, G., Stuchlík Z., Šrámková, E., 2007, in preparation
Barret D., Olive J.-F., Miller M. C., 2005c, MNRAS, 361, 855
Belloni, T., Méndez, M., Homan, J., 2005, A&A 437, 209
Belloni, T., Méndez, M., Homan, J., 2007, MNRAS, accepted
Bradt, H. V., Rothschild, R. E., Swank, J. H. 1993. X–ray timing explorer mission. Astronomy and Astrophysics Supplement Series 97, 355-360.
Bursa, M., in Proceedings of RAGtime 6/7, eds. S. Hledík, Z. Stuchlík, Opava, 2005
Giles, A. B., Hill, K. M., Strohmayer, T. E., Cummings, N., 2002, ApJ, volume 568, part 1 (2002), pages 279-288
Glendenning, N., K., Compact Stars: Nuclear Physics, Particle Physics, and General Relativity, Springer-verlag New York, Inc., 1997
Hartle, J.B, Thorne, K.S., 1968, APJ, 153
Kluźniak, W., & Abramowicz, M. A., 2000, Phys. Rev. Lett. (submitted); see also Kluźniak, W., & Abramowicz, M. A., 2001, Acta Physica Polonica B 32, 3605 [http://th-www.if.uj.edu.pl/acta/vol32/t11.htm]
Kluźniak, W., Abramowicz, M.A., 2001, astro-ph/0105057
Landau, L. D., & Lifshitz, E. M., 1976, Mechanics, 3rd edition, (Oxford: Pergamon Press)
Marquardt, D.W., 1963, Journal of the Society for Industrial and Applied Mathematics, 11, 431
McClintock, J. E, & Remillard, R. A., in Compact Stellar X-ray Sources, eds. W.H.G. Lewin and M. van der Klis, Cambridge University Press, 2004, astro-ph/0306213; see also McClintock, J. E, & Remillard, R. A., 2006, Annual Review of A&A, 44, 1, pp.49-92, astro-ph/0606352
McClintock, J. E., Shafee, R., Narayan, R., et al. 2006, Astrophys. J., 652, 518, astro-ph/0606076
Middleton, M., Done, C., Gierliński, M., & Davis, S. W. 2006, MNRAS, 373, 1004, astro-ph/0601540
Méndez, M., van der Klis, M., Wijnands, R., Ford, E. C., van Paradijs, J., Vaughan, B. A., 1998, ApJ, 505, L23
Misner, Ch., W., Thorne, K., S., Wheeler, J., A., Gravitation, San Francisco: W.H. Freeman and Co., 1973
Okazaki, A. T., Kato, S., & Fukue, J. 1987, Publ. Astron. Soc. Japan, 39, 457
Rebusco, P., 2004, PASJ 56, 533
Shapiro, S. L., Teukolsky, S. A., Black Holes, White Dwarfs and Neutron Stars: The Physics of Compact Objects, Wiley-VCH, 1986
Stella, L. & Vietri, M. 1998, Astrophys. J., 492, L59
Stella, L. & Vietri, M. 1999, Phys. Rev. Lett., 82, 17
Strohmayer, T. E., Markwardt, C. B., 2001, ApJ, Volume 577, Issue 1, pp. 337-345
Stuchlík, Z., Török, G., 2005, in Proceedings of RAGtime 6/7, eds. S. Hledík, Z. Stuchlík, Opava, 2005
Stuchlík, Z., Kotrlová, A., Török, G., 2007, in preparation
Török, G., Abramowicz, M.A., Kluźniak, W. & Stuchlík, Z. 2005, A&A 436, 1
Török, G., & Stuchlík, Z., 2005, A&A, volume 437, p.775-788, astro-ph/0502127
Török, G., Barret, D., A$A, 2007, to be submitted
Török, G., Stuchlík, Z., Bakala P., MNRAS, 2007, submitted
van der Klis, M., In Compact stellar X-ray sources, eds. W. Lewin & M. van der Klis., Cambridge University Press, 2006, p. 39

Appendix A: Formulae for orbital geodesic frequencies in the Hartle–Thorne metric

After Abramowicz et al. (2003a), the Keplerian orbital angular velocity and the radial and vertical epicyclic angular velocities can be expressed in terms of the Hartle-Thorne metric parameters M, j, , q in the following form.

The angular velocity for corotatingcircular particle orbits reads

$$\Omega_K = u^\phi/u^t = \frac{M^{1/2}}{r^{3/2}}\left[1 - j\,\frac{M^{3/2}}{r^{3/2}} + j^2\,F_1^{\Omega}(r) + q\,F_2^{\Omega}(r)\right], \tag{A.1}$$

where

$$F_1^{\Omega}(r) = \left[48\,M^7 - 80\,M^6\,r + 4\,M^5\,r^2 - 18\,M^4\,r^3 + 40\,M^3\,r^4 + 10\,M^2\,r^5 \right. \tag{A.2}$$
$$\left. +15\,M\,r^6 - 15\,r^7\right]\,(16\,M^2\,(r-2M)\,r^4)^{-1} + H(r)$$

$$F_2^{\Omega}(r) = \frac{5\left(6\,M^4 - 8\,M^3\,r - 2\,M^2\,r^2 - 3\,M\,r^3 + 3\,r^4\right)}{16\,M^2\,(r-2M)\,r} - H(r) \tag{A.3}$$

$$H(r) = \frac{15\left(r^3 - 2\,M^3\right)}{32\,M^3}\,\ln\left(\frac{r}{r-2M}\right). \tag{A.4}$$

The epicyclic frequencies of circular geodesic motion are given by formulae

$$\omega_r^2 = \frac{M(r-6M)}{r^4}\left[1 + j\,H_1(r) - j^2\,H_2(r) - q\,H_3(r)\right] \tag{A.5}$$

$$\omega_\theta^2 = \frac{M}{r^3}\left[1 - j\,I_1(r) + j^2\,I_2(r) + q\,I_3(r)\right] \tag{A.6}$$

where

$$H_1(r) = \frac{6\,M^{3/2}\,(r+2M)}{r^{3/2}\,(r-6M)} \tag{A.7}$$

$$H_2(r) = \left[8M^2\,r^4\,(r-2M)\,(r-6M)\right]^{-1}\left[384M^8 - 720M^7r - 112M^6r^2 - 76M^5r^3\right.$$
$$\left. - 138M^4r^4 - 130M^3r^5 + 635M^2r^6 - 375Mr^7 + 60r^8\right] + J(r) \tag{A.8}$$

$$H_3(r) = \frac{5\,(48M^5 + 30M^4r + 26M^3r^2 - 127M^2r^3 + 75Mr^4 - 12r^5)}{8M^2\,r\,(r-2M)\,(r-6M)} - J(r) \tag{A.9}$$

$$I_1(r) = \frac{6\,M^{3/2}}{r^{3/2}} \tag{A.10}$$

$$I_2(r) = \left[8M^2\,r^4\,(r-2M)\right]^{-1}\left[48M^7 - 224M^6r + 28M^5r^2\right.$$
$$\left. + 6M^4r^3 - 170M^3r^4 + 295M^2r^5 - 165Mr^6 + 30r^7\right] - K(r) \tag{A.11}$$

$$I_3(r) = \frac{5\left(6M^4 + 34M^3r - 59M^2r^2 + 33Mr^3 - 6r^4\right)}{8M^2\,r\,(r-2M)} + K(r), \tag{A.12}$$

with

$$J(r) = \frac{15r\,(r-2M)\,(2M^2 + 13Mr - 4r^2)}{16M^3\,(r-6M)}\,\ln\left(\frac{r}{r-2M}\right) \tag{A.13}$$

$$K(r) = \frac{15\,(2r-M)\,(r-2M)^2}{16M^3}\,\ln\left(\frac{r}{r-2M}\right). \tag{A.14}$$

For completness, the relation determining the marginally stable circular geodesic reads

$$r_{\rm ms} = 6\,M\left[1 - j\,\frac{2}{3}\sqrt{\frac{2}{3}} + j^2\left(\frac{251647}{2592} - 240\,\ln\,\frac{3}{2}\right) + q\left(-\frac{9325}{96} + 240\,\ln\,\frac{3}{2}\right)\right]. \tag{A.15}$$